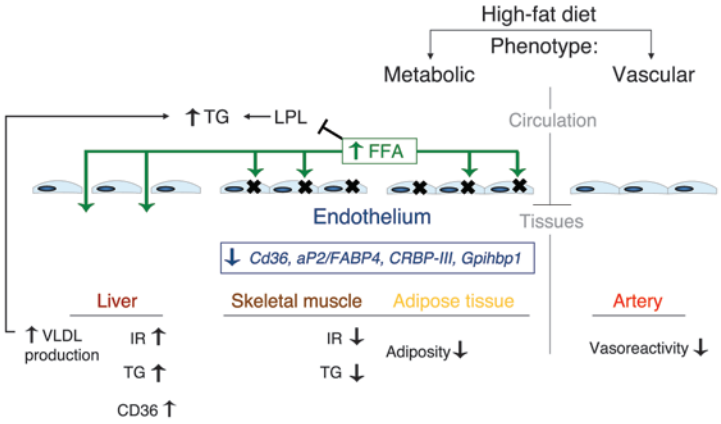

Figure 12

PPARγ in the endothelium integrates metabolic and vascular phenotypes. Studies in mice lacking PPARγ in the endothelium identify endothelial PPARγ as controlling specific metabolic and vascular responses to high-fat diet, as summarized. After high-fat diet feeding, mice lacking endothelial PPARγ manifest increased plasma TG and FFA levels, decreased adiposity, less skeletal muscle TG accumulation, and decreased insulin resistance (IR). This phenotype derives from endothelial PPARγ regulation of target genes involved in TG metabolism as well as FA uptake and handling, including *Cd36*, *aP2*, *CRBP-III*, and *Gpihbp1*. In contrast, livers in endothelial PPARγ-deficient mice have greater TG accumulation, increased VLDL production, and decreased AKT phosphorylation. In the liver, the endothelium is fenestrated, which fosters FFA uptake, while in skeletal muscle and adipose tissue, a nonfenestrated endothelium is found. The dyslipidemia seen in endothelial PPARγ-deficient mice after high-fat diet and acute lipid loading involves both increased VLDL production and inhibition of LPL function by elevated FFA levels. The metabolic improvements evident in endothelial PPARγ-deficient mice contrast with their impaired arterial vasodilation, highlighting the tissue-specific actions of endothelial PPARγ, the role of the endothelium in directing metabolic responses, and the concept of metabolic endothelial function/dysfunction.

multilocular adipocytes in adipose tissue (19), although others have not found such effects (20). In the Tie2Cre model, neither the presence nor absence of PPARγ in BM (γEC-WT/BM-WT or γEC-WT/BM-KO mice, respectively; Figures 5 and 6) altered fat accumulation. The impact of hematopoietic PPARγ on adiposity requires further investigation.

More specifically, PPARγ deletion in macrophages has been reported to increase adiposity and promote insulin resistance in a high-fat diet–fed model (56, 57). We did not observe worsening insulin resistance despite Tie2-mediated PPARγ deletion in hematopoietic cells. Other studies reported that Tie2-mediated PPARγ deletion increased osteopetrosis and resulted in inflammatory maternal milk (14, 58). Strain differences may contribute to these variable findings, as suggested by recent work that also reported no effect of macrophage PPARγ on insulin sensitivity exists (59). Variations in the dietary stimulation used in these studies may also contribute to the differences seen. Of note, both γEC/BM-KO and γEC/BM-WT mice have predominant noninflammatory monocyte subsets (data not shown), a factor recently implicated in atherosclerosis (60), obesity (61), and insulin resistance (56). In terms of inflammation, we did not observe significant differences in TNF-α and IL-6 levels in adipose tissue (data not shown). The time course of macrophage infiltration into adipose tissue may also factor into the impact of hematopoietic PPARγ deletion on insulin resistance. Inflammatory macrophages are recruited to adipose tissue in later stages of obesity; our studies were done after approximately 12 weeks of high-fat diet, when macrophage infiltration is less obvious (62).

Taken together, we demonstrate here that endothelial PPARγ integrates both metabolic and vascular responses. In the presence of endothelial PPARγ deletion, FFA levels, TG-rich lipoprotein metabolism, adiposity, and insulin sensitivity in response to high-fat diet or an oral lipid challenge are altered. Prior studies in this same Tie2Cre model of PPARγ deletion have shown that high-fat diet induces hypertension (11). In that prior report and our studies here, changes through endothelial PPARγ were particularly evident in response to high-fat diet, emphasizing the importance of PPARγ in the handling of fat and FAs that are commonly encountered in Western diets. Although endothelial PPARγ-deficient mice are protected against increased adiposity and insulin resistance, they still manifest abnormal vasodilatory responses, effectively disassociating the role of endothelial PPARγ in metabolism from its local effect on the arterial wall. In so doing, a more precise and expansive systemic role for the endothelium is evident. In humans, endothelial dysfunction occurs early in the natural history of obesity and diabetes, often preceding frank hyperglycemia (2, 3). Indeed, endothelial dysfunction can be found disproportionately among young, normotensive first-degree relatives of those with diabetes (63). The evidence provided here implicating PPARγ in the endothelium in directing metabolic phenotype and therapeutic responses argues that our understanding of endothelial action may need to be extended to include concepts of metabolic endothelial function and dysfunction.

Methods

Mice. PPARγ-floxed and Tie2Cre mice, as previously described, are of mixed C57BL6/N;Sv129;FVB/N background (11). Using sibling matings (γEC/BM-KO males and γEC/BM-WT females), mice were bred for at least 12 generations before studies on male γEC/BM-KO and γEC/BM-WT mice. All mice were housed on a 12-hour light/dark cycle, with food and water ad libitum. Animal care and experimentation was approved by the Harvard Medical School Institutional Animal Care and Use Committee.

Before study, all mice were fed a standard pellet diet (13.2% calories from fat; PicoLab Rodent 20 no. 5053, Lab Diet Inc.). Obesity was induced using a high-fat diet (60% calories from fat; D12492, Research Diets Inc.) for 12–27 weeks, beginning at 6 weeks of age. Low-fat diet–fed mice received the standard pellet diet throughout life. For rosiglitazone experiments, mice were fed standard diet (AIN-76A Rodent Diet, Research Diets Inc.), with or without 130 mg rosiglitazone/kg diet (ad libitum, 5 weeks; GlaxoSmithKline). The rosiglitazone dose was determined by pilot dose ranging studies. For olive oil gavage experiments with rosiglitazone, mice were fed the AIN-76A diet, with or without 70 mg rosiglitazone/kg diet (ad libitum, 3 weeks).

Mouse EC isolation. Microvascular ECs were isolated from mouse hearts (at 1 month of age), using ICAM-2 and PECAM-1 antibody (BD Biosciences — Pharmingen) Dynabead selection as described before (64).

RNA analysis. DNase I–treated total RNA was reverse transcribed, and real-time quantitative PCR with cDNA was performed using SYBR Green I (iCycler iQ Real-Time PCR Detection System; Bio-Rad). Sense and antisense cDNA primers, respectively, were as follows: *Pparg*, 5′-CAAGAATACCAAAGTGCGATCAA-3′, 5′-GAGCAGGGTCTTTTCAGAATAATAAG-3′; *Cd36*, 5′-GGCCAAGCTATTGCGACAT-3′, 5′-CAGATCCGAACACAGCG-